Pol J Med Phys Eng 2010;16(1):11-21.
PL ISSN 1425-4689
doi: 10.2478/v10013-010-0002-z
website: http://www.pjmpe.waw.pl

Mohammed A. Al Asmary[1], Manickam Ravikumar[2]

Position of effective electron source for shielded electron beams from a therapeutic linear accelerator

[1]Medical Physics Department, Oncology Center, King Abdul Aziz Hospital and Oncology Center, Jeddah 21456, Saudi Arabia
[2]Department of Radiation Physics, Kidwai Memorial Institute of Oncology, Bangalore, India
e-mail: alasmr@hotmail.com

The effective electron source positions for the standard electron cones and for the shielded field sizes with cerrobend inserts were measured based on Inverse Square Law (ISL) and the Inverse Slope (IS) method for various electron energies.

The charge measurements were carried out using a 0.6 cc ion chamber (PTW, Type 30001) connected to a PTW Unidos E digital electrometer in a polystyrene phantom for electron beam energies of 6-18 MeV. The resultant charge for 100 MU setting was measured at nominal source to surface distances (SSDs) of 100-120 cm for cone and cerrobend defined field sizes.

The effective SSD (SSD_{eff}) was found to be different for the same field size defined by electron applicator and the cerrobend shield placed in 25×25 cm standard cone. Strong dependency of SSD_{eff} with field size and electron beam energy was noticed.

The results from the ISL and IS method are consistent, hence either of the two methods can be used to determine the effective source position. Whenever treatment is to be given with shielded electron portal, the SSD_{eff} for that field needs to be determined. Same SSD_{eff} as that of the standard cone can be used for minimum shielded electron portals.

Key words: electron beam, effective electron source, inverse square law, inverse slope.

Introduction

The superficial and shallow tumors are usually treated with cerrobend shielded electron beams. The irregular field defining inserts are placed at the distal end of the electron applicators. Due to the curved and irregular body surfaces, most of the patients are treated at an extended source-to-surface distances (SSDs). When the treatment is delivered at an extended distance, the electron output and the percentage depth dose needs to be corrected based on inverse square law from the electron source position. As the electron beam emerging from an accelerator exit window undergoes complex multiple scattering in the scattering foil, the beam monitor chambers, the X-ray collimators, electron applicators, field defining inserts and air column, the position of scattering foil can not be considered as a nominal source position and the output corrected accordingly. In such cases the output can be predicted accurately assuming the effective or virtual source position and the inverse square law applied to the effective SSD. The International Commission on Radiation Units and Measurements (ICRU) defines [6] the effective source as the source which when placed in vacuum at some distance SSD from the phantom surface ($Z=0$) produces the same electron fluence at $Z=0$ as the real beam. The effective SSD is the distance between the effective source positions to the patient skin surface. It is a function of beam energy, field size and the method of collimation [2, 7-9, 11].

Though the effective point source position can be estimated using Full-Width Half Maximum (FWHM) method [5, 8, 10] and the Multi Pin-hole Camera (MPC) method [13], the results from these measurements are consistent only for large fields and for energies greater than 15 MeV [7]. The Inverse Square Law (ISL) method [1], the Inverse Slope (IS) method [9] and the Power Law (PL) method [15] are usually the preferred methods as they simulate the clinical conditions encountered. It was reported that the results obtained from the ISL method are consistent with those based on PL method for all electron energies and field sizes [7].

As the scattering and the field defining geometry vary with different accelerators, the effective position of the source must be determined for each individual accelerator [3-4, 7, 9, 12, 14, 17]. In the present study the effective electron source positions were determined for field sizes defined by the standard electron cones supplied by the manufacturer and for the shielded field sizes with cerroband inserts in the standard cone for various electron energies.

Materials and methods

The study was carried out with electron beams of nominal energies 6, 8, 10, 12, 15 and 18 MeV from Mevatron KDS (Siemens, Germany) linear accelerator at a dose rate of 300 MU/min. The standard applicators supplied by the manufacturer can define a circular field of 5 cm diameter and a square field of 10×10 cm to 25×25 cm at isocenter with the photon jaw settings as shown in Table 1. Shielded Circular field of 5 cm diameter and the square field sizes of 10×10, 15×15 and 20×20 cm were machined for the 25×25 cm standard applicator.

Table 1. The collimator jaw settings for different standard applicators

Applicator size [cm^2]	Collimator opening [cm^2] for electron energy [MeV]					
	6	8	10	12	15	18
5∅	13×13	13×13	13×13	13×13	13×13	13×13
10×10	19×19	19×19	19×19	19×19	19×19	19×19
15×15	23×23	23×23	23×23	23×23	23×23	23×23
20×20	27×27	27×27	27×27	27×27	27×27	27×27
25×25	32×32	32×32	32×32	32×32	32×32	32×32

The charge measurements were carried out using a 0.6 cc Farmer type ion chamber (PTW, Type 30001) connected to a PTW Unidos E digital electrometer at a bias voltage of +400 V. The chamber was positioned with its effective point of measurement (0.5 r upstream from the center towards the source) at the depth of maximum in a 30×30×30 cm^3 Water equivalent RW3 slab phantom (PTW T29672). The resultant charge for 100 MU setting was measured at nominal source to surface distances (SSDs) of 100, 105, 110, 115 and 120 cm. To find out the SSD_{eff} based on inverse square law method [1] a plot was made between the nominal SSD and the square root of the inverted charge for each energy and field size combinations. If the data forms a straight line, the inverse square law (ISL) is applicable and if the straight line passes through zero, the effective source is at the same position as that of the scattering foil (100 cm).

The extrapolation of the curve back to the abscissa yields the effective source position. The straight line with a positive intercept indicates that the effective source is downstream the scattering foil while a negative intercept implies that the source is upstream the scattering foil. The effective SSD was also evaluated based on Khan's [9] inverse slope method, for which a graph was drawn with the square root of the charge ratio, $\sqrt{\frac{Q_0}{Q_g}}$, on y-axis where Q_0 is the collected charge with no air gap (100 cm nominal SSD) and Q_g is the collected charge with air gap g, and air gap g on x-axis. When a least square fit is drawn to the graph the slope of the resulting line is the reciprocal of the $SSD_{eff+dmax}$. Hence the effective SSD can be obtained from an equation

$$\mathrm{SSD} = \frac{1}{\mathrm{slope}} - d_{\max} \quad . \tag{1}$$

Results

The graphs drawn between the nominal SSD and the square root of the inverted charge for 6, 12 and 18 MeV electron energies for 5 cm diameter and 20×20 cm standard cones are shown in Figures 1a and 1b. The straight line with a positive intercept in Figure 1a indicates that the effective source is downstream the scattering foil with SSD_{eff} less than 100 cm, and the negative intercept in Figure 1b implies that the source is upstream with SSD_{eff} greater than 100 cm. The plot made between the square root of the charge ratio, $\sqrt{\frac{Q_0}{Q_g}}$, and air gap g for 8, 10 and 15 MeV electron energies for 5 cm diameter and 20×20 cm standard cones are shown in Figures 2a and 2b. The slope for the resulting straight line is obtained and the SSD_{eff} evaluated using equation (1). The measured effective SSDs using ISL and IS method for the standard cones supplied by the manufacturer and the cerroband cut-out defined field sizes are shown in Tables 2 and 3 for various electron energies. The SSD_{eff} was found to change with electron energies and the standard applicator (Figure 3). The effective SSDs for the cutout defined fields in a 25×25 cm cone were noticed to differ from that of the standard 25×25 cm cone dimension (Figure 4).

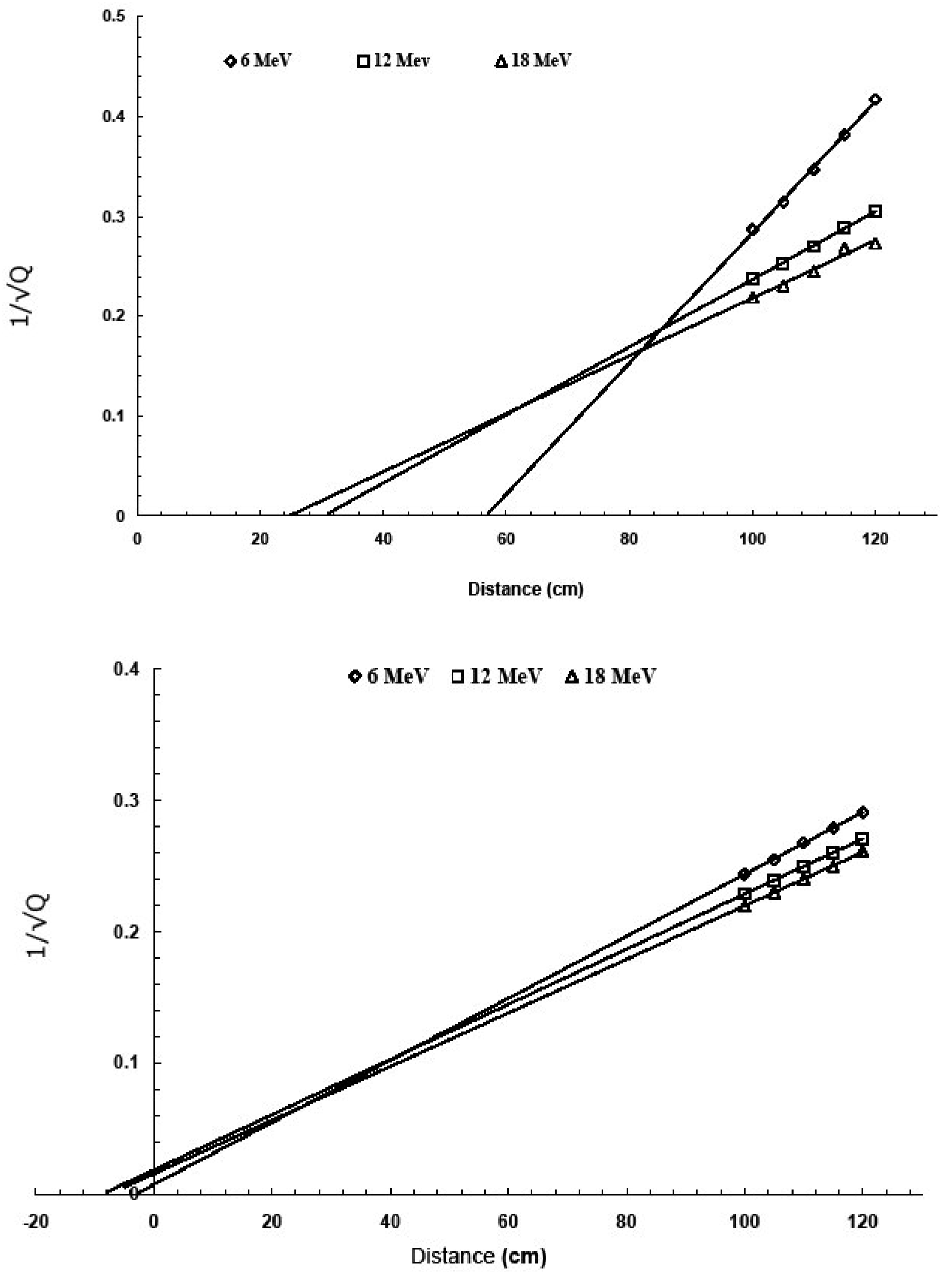

Figure 1. Variation between the nominal SSD and the square root of the inverted charge for 6, 12 and 18 MeV electron energies for: a) 5 cm diameter and b) 20 cm square standard cones.

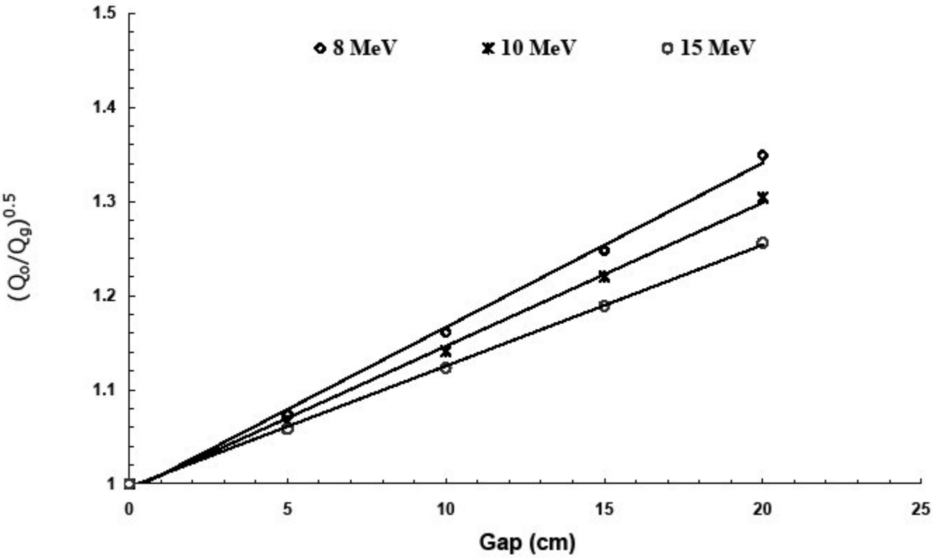

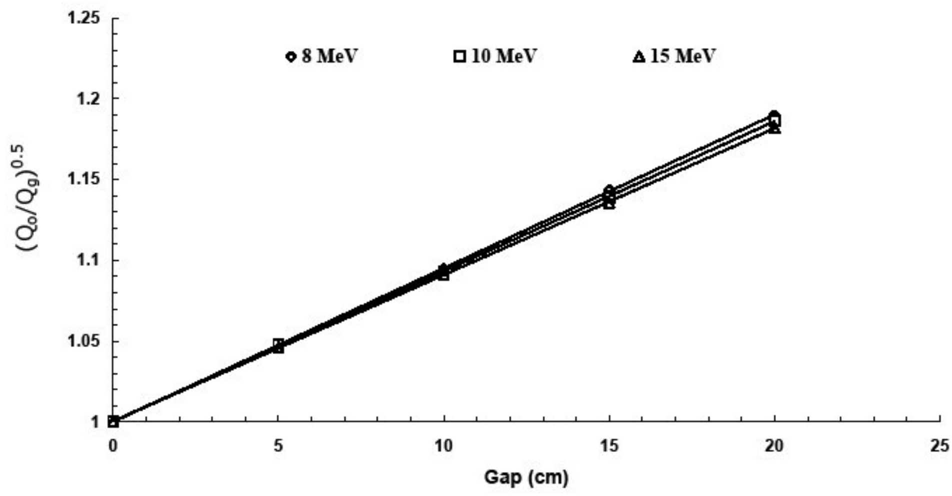

Figure 2. Variation between the square root of the charge ratio and air gap *g* for 8,10 and 15 MeV electron energies for: a) 5 cm diameter circular and b) 20 cm square standard cones.

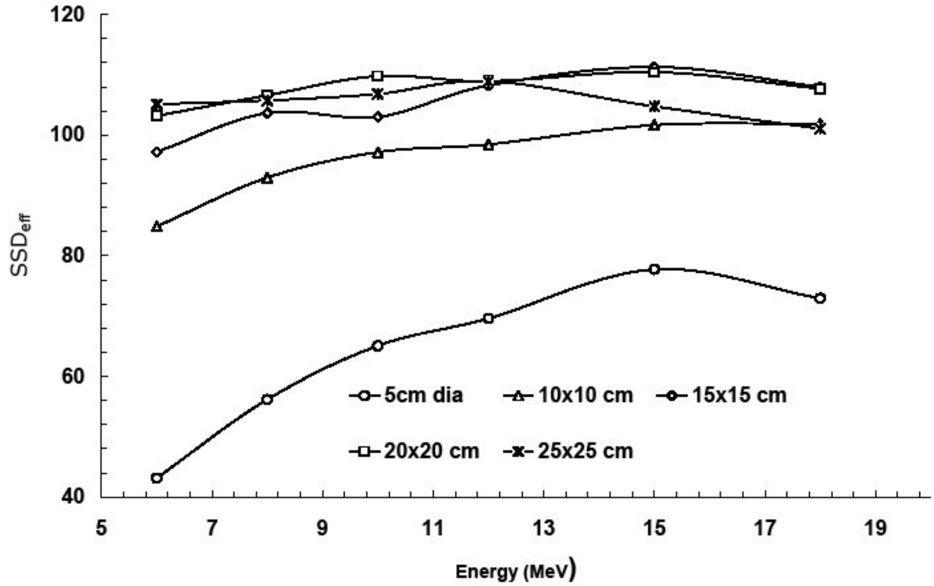

Figure 3. Variation of SSD_{eff} for standard cones at different electron energies.

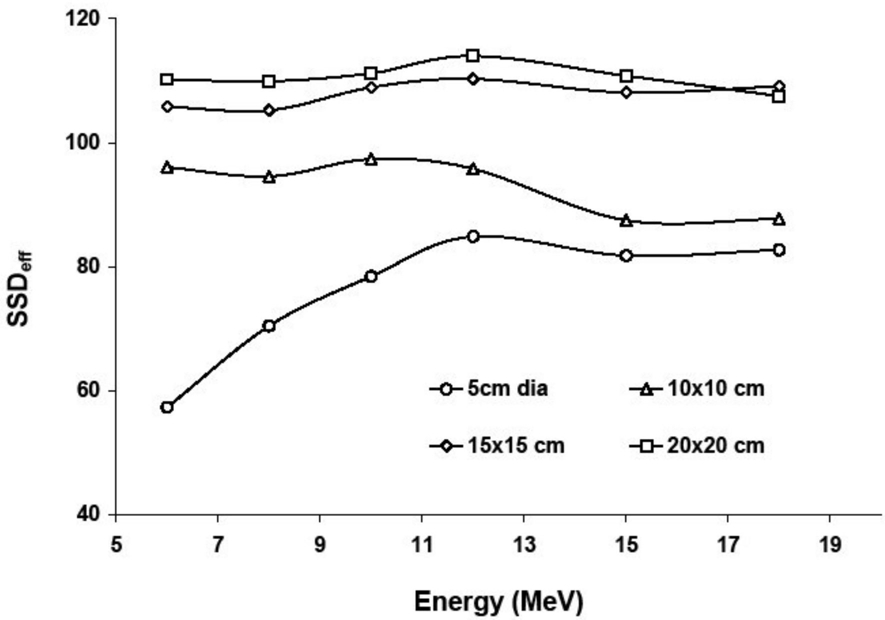

Figure 4. Variation of SSD_{eff} for cerrobend defined fields at different electron energies.

Table 2. The measured effective SSDs using Inverse Square Law (ISL) and Inverse Slope (IS) methods for standard applicators

Applicator size [cm^2]	Electron energy [MeV] and methods for standard applicators											
	6		8		10		12		15		18	
	ISL	IS	ISL	IS	ISL	IS	ISL	IS	ISL	IS	ISL	IS
5∅	43.1	42.1	56.2	55.6	65.1	63.5	69.6	68.3	77.7	75.8	72.9	74.5
10×10	84.9	84.2	92.9	91.3	97.2	96.5	98.5	97.9	101.7	99.34	101.9	100.7
15×15	97.2	97.3	103.7	100.6	103	102.6	108.2	107.1	111.3	107	108	106
20×20	103.2	101.9	106.6	103.3	109.8	105.5	108.9	107.6	110.4	107.9	107.7	106.7
25×25	105.1	103.7	105.8	104.4	106.8	106.6	108.9	107.1	104.7	102.1	101.2	101.1

Table 3. The measured effective SSDs using Inverse Square Law (ISL) and Inverse Slope (IS) methods for Cerroband insert cut-out fields

Applicator size [cm^2]	Electron energy [MeV] and methods for insert cutout fields											
	6		8		10		12		15		18	
	ISL	IS	ISL	IS	ISL	IS	ISL	IS	ISL	IS	ISL	IS
5∅	57.3	57.5	70.4	69.3	78.4	76.2	84.9	81.8	81.8	80.4	82.7	81.6
10×10	96	95.2	94.6	94.4	97.3	97.1	95.8	96.6	87.5	86.1	87.7	86.6
15×15	105.8	105.5	105.2	105	108.9	105.9	110.3	107.5	108.1	107.6	109.1	105.5
20×20	110.2	107.4	109.9	108.1	111.2	110.3	114	111	110.8	111.3	107.5	105.9

Discussion

The results based on ISL and IS method for the estimation of SSD_{eff} shows a strong field size and energy dependency (Table 2 and 3). For smaller field sizes the SSD_{eff} are much lesser and this is due to the lack of side scatter equilibrium [9, 11, 16]. For higher energy electrons (beyond 12 MeV) the 5 cm shielded circular field has higher SSD_{eff} value compared to that of low energy electrons and this could be attributed due to the presence of less side scattering and more forward scattering. Since the side scatter equilibrium exists for larger field sizes, no variation in effective SSD is noticed for field sizes greater than 15×15 cm. The change in SSD_{eff} values for the same field opening with the standard applicator and the field defined by the insert in a larger applicator could be due to the difference in scattering pattern arising from the photon collimators and the electron cones. As the photon collimator opening is more for 25×25 cm applicator (32×32 cm) compared to that of the other applicators, there exists more scatter from the larger surface area of the collimators towards the central axis resulting in higher fluence. The results from the ISL and IS method are quite consistent within acceptable limits, either of the two methods can be used to determine the effective source position.

Conclusion

The effective SSD (SSD_{eff}) varies considerably between the applicator and cutout defined fields. Whenever treatment is to be given with shielded electron portal, the SSD_{eff} for that field needs to be determined. However when the treatment portal with minimum shielding in a large standard applicator is used the same SSD_{eff} of the standard applicator can be used to find out the correction factors.

Acknowledgement

The authors wish to acknowledge Mr. Salim Hasan Salim Abdulslam, Chief Radiotherapist at King Abdul Aziz Hospital and Oncology Center for his experimental assistance and for machining the cerrobend blocks.

References

[1] Almond PR. Radiation Physics of Electron Beams. In: Tapley N, editor. Clinical Applications of the Electron Beams. New York: John Wiley & Sons; 1976. p. 7-80.

[2] Cecatti ER, Goncalves JF, Cecatti SG, da Penha Silva M. Effect of the accelerator design on the position of the effective electron source. Med Phys. 1983 Sep-Oct;10(5):683-686.

[3] Faermann S, Krutman Y, Weinstein M. A Comparison of the method of determination of virtual sources for electron beams. Proc. of the 5th Clinac User's Meeting; USA. 1983.

[4] Al-Ghazi MS, Lingman D, Arjune B, Gilbert LD, Thekkumthala J. Characteristics parameters of 6-21 MeV electron beams from a 21 MV linear accelerator. Med Phys. 1991;18:821-828.

[5] Hogstrom KR. Evaluation of electron pencil beam dose calculation. Med Phys. 1985;12:554-557.

[6] ICRU REPORT 35. Radiation Dosimetry: Electron Beams with Energies Between 1 and 50 MeV. 1984.

[7] Jamshidi A, Kuchnir FT, Reft CS. Determination of the source position for the electron beams from a high energy linear accelerator. Med Phys. 1986;13:942-945.

[8] Khan FM. Clinical electron beam dosimetry. Proceedings of the 1986 Summer School of the AAPM. New York (NY): p. 194-246.

[9] Khan FM, Sewchand W, Levitt SH. Effect of airspace on depth dose in electron beam therapy. Radiology. 1978;126:249-251.

[10] Meyer J, Palta J, Hogstrom K. Demonstration of relatively new electron dosimetry measurement techniques on the Mevatron 80. Med Phys. 1984 Sep-Oct;11(5):670-677.

[11] Mills MD, Hogstrom KR, Almond PR. Prediction of electron beam output factors. Med Phys. 1982 Jan-Feb;9(1):60-68.

[12] Ravikumar M, Ravichandran R. Effect of shielding on virtual source position for electron beams from a Clinac-1800 linear accelerator. J Med Phys. 1999;24:21-24.

[13] Schroder-Babo P. Determination of the virtual electron sources of a betatron. Acta Radiol. 1983; 364(suppl):7-10.

[14] Sharma AK, Supe SS, Sathiya Narayanan VK, Subbarangaiah K. Determination of virtual SSDs for electron beams from a dual energy linear accelerator. Strahlenther Onkol. 1992 Jul;168(7):402-405.

[15] Sweeney LE, Gur D, Bukovitz AG. Scatter component and its effect on virtual source and electron beam quality. Int J Radiat Oncol Biol Phys. 1981 Jul;7(7):967-971.

[16] Khan FM, Doppke KP, Hogstrom KR, Kutcher GJ, Nath R, Prasad SC et al. Clinical electron-beam dosimetry: report of AAPM Radiation Therapy Committee Task Group No. 25. Med Phys. 1991 Jan-Feb;18(1):73-109.

[17] Thomadsen BR, Asp LW, Van de Geijn J, Paliwal BR, PoCheng C. Perturbation of electron beam doses as a function of SSD due to the use of shielding blocks on the Clinac-18. Med Phys. 1981 Jul-Aug;8(4):507-509.